

We are IntechOpen, the world's leading publisher of Open Access books Built by scientists, for scientists

4,800

Open access books available

122,000

International authors and editors

135M

Downloads

Our authors are among the

154

Countries delivered to

TOP 1%

most cited scientists

12.2%

Contributors from top 500 universities



WEB OF SCIENCE™

Selection of our books indexed in the Book Citation Index
in Web of Science™ Core Collection (BKCI)

Interested in publishing with us?
Contact book.department@intechopen.com

Numbers displayed above are based on latest data collected.
For more information visit www.intechopen.com



Steam Turbines Under Abnormal Frequency Conditions in Distributed Generation Systems

Fabrício A. M. Moura¹, José R. Camacho²,
Geraldo C. Guimarães² and Marcelo L. R. Chaves²

¹*Federal University of Triângulo Mineiro,*

²*Federal University of Uberlândia,
Brazil*

1. Introduction

Considerable efforts have been developed to encourage the installation of independent electricity producers in distribution systems. Obvious example of such efforts is demonstrated by the attempt to standardize their interconnection and protection requirements. However, this standardization can be difficult due to variations in the design of distribution circuits, the various types of generators coupled to the network and the particular requirements of each utility. However, a series of questions points to the development of further studies to ensure the quality of electric power, the system transient stability and lifetime of the blades of steam turbines (Moura et al., 2011).

Distributed generation shows frequent use of steam turbines as a primary machine to produce electricity. Such units have increased considerably due to a restructuring of the energy sector worldwide.

Most of the process of converting thermal energy into electrical energy occurs in the steam turbine. This is due to the numerous advantages of such turbines over other similar technologies. Among the main advantages stands the balanced construction, relatively high efficiency, few moving parts, ease of maintenance, and availability in large sizes. The industries that typically employ the technology of cogeneration are the sugar and ethanol, the pulp and paper and oil refining (Anderson & Fouad, 2003).

Recently, special attention has been devoted to turbo-alternators under abnormal conditions of operation of the electrical system concerning the frequency (over or under frequency). In particular, major research efforts have been spent with the main aim of assessing the possible damage they are subjected to the steam turbine when in operation under conditions of prolonged under frequency, during a severe overload condition imposed on the system when occurring a deficit of generation (Kundur, 1994).

Contingencies common to the distribution of electricity systems can cause serious damage to the generators installed in parallel to the network as well as steam turbines responsible for providing mechanical power to their axis. Thus, it is necessary to assess the possible impacts of steam turbines of the IP (independent producer) electrical machinery in system abnormal operating conditions.

For this it is essential to develop a computer model able to represent accurately the phenomena experienced.

2. Steam turbines control functions

The speed regulation system is the primary control loop of the Automatic Generation Control (AGC) of an electrical system. The control of active power in a power system is accomplished primarily by controlling the torque of the machines primary drive system (Anderson & Fouad, 2003).

Figure 1 illustrates a system for regulating the speed of a steam turbine. By controlling the position x_E of the control valve, a control can be exercised over the admission of steam (or water) at high pressure through the turbine, and therefore the torque of the turbine. For a hydraulic amplifier, the input is the position of the pilot valve x_D and the output is position x_E of the main piston. A small downward movement of point E, the steam flow increases by an amount that, if measured in terms of power valve, represents an increment ΔP_v . This increased flow is rendered by the increase in turbine power, ΔP_t .

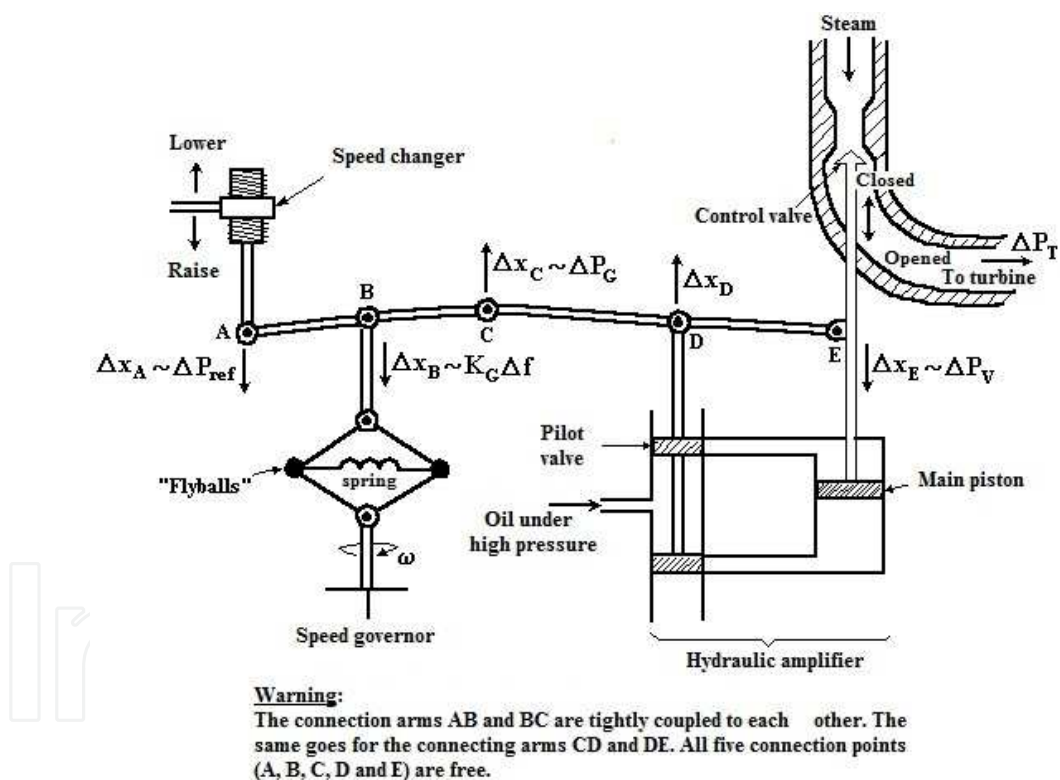


Fig. 1. Example illustrating the mechanical speed control system of a steam turbine

The pilot valve x_D , still in figure 1, can have its position changed, through the links or arms connection system, in three ways:

- Directly, by the speed changer. A small downward movement of the connecting point A (Δx_A) corresponds to an increase in the reference power, ΔP_{ref} ;
- Indirectly, by feedback, due to changes in the position of the connection point E of the main piston (Δx_E), resulting from variations in steam pressure;

- Indirectly, by feedback due to changes in the position of the connection point B (Δx_B), resulting from changes in speed.

Historically, *load-frequency primary controls* are part of the so-called *characteristics of speed governors*. However, the term “regulator” implies a mechanical speed sensor mechanically connected to control variations in input power, and since today most of the load-frequency controls are electro-hydraulic, speed control term does not describe generically this control function (Kundur, 1994).

2.1 Isochronous governor

Another simple mechanism of regulation is shown by figure 2. In this case, the deviation in speed, captured by the centrifugal body (*flyballs*), cause the displacement Δx in the pilot valve, which makes the oil to flow through the main servo motor. This servo motor, in turn, opens or closes the valve or turbine blades, depending on the direction of Δx .

It is important to observe that a displacement Δx in the pilot valve causes a rate of change of the servo piston, or a rate of change in the valve position.

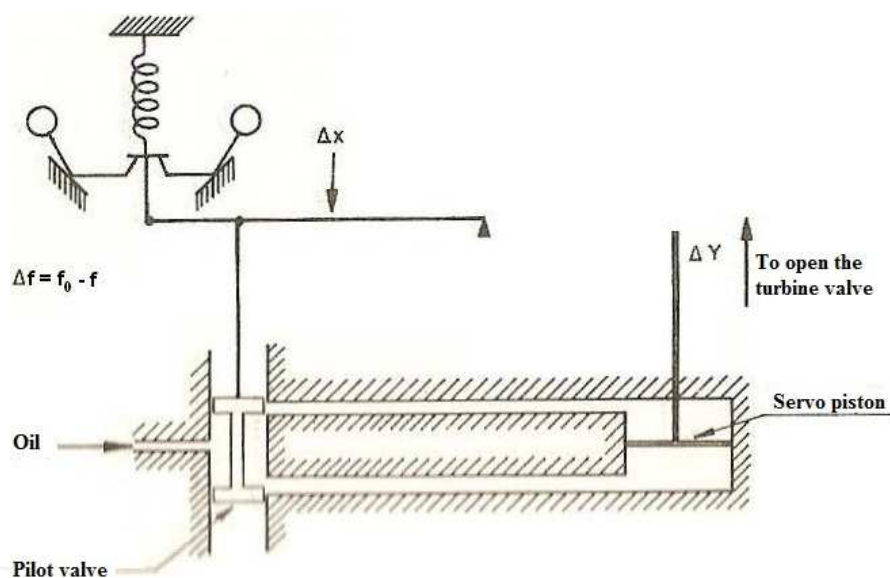


Fig. 2. “Isochronous” type speed governor

With reference to figure 2, can be written for the position of pilot valve (Δx):

$$\Delta x = k_1 \Delta f \quad (1)$$

where:

Δf = frequency deviation ($f_0 - f$);

k_1 = proportionality constant.

Also, for the turbine valve position (Δy), we have:

$$\frac{d}{dt}(\Delta y) = k_2 \Delta x \quad (2)$$

where:

k_2 = proportionality constant.

$$\frac{d}{dt}(\Delta y) = k_1 k_2 \Delta f$$

or

$$\Delta y = \int k_1 k_2 \Delta f dt \quad (3)$$

These equations are described in the block diagram in figure 3.

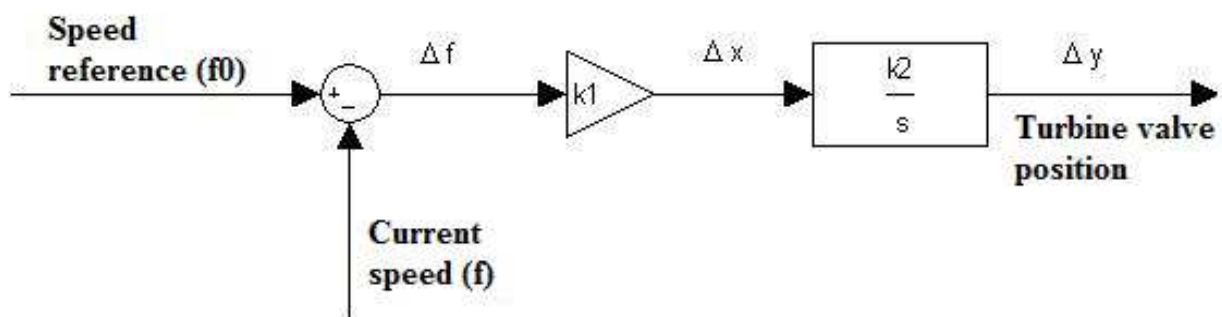


Fig. 3. Block diagram of the isochronous type speed governor

Due to the integrative action of the main servo motor, it is evident that Δy reach a new equilibrium state only when Δf reaches zero.

The governor with the configuration of figure 2 will therefore reduce the frequency error to zero in steady state and move the valve position, within physical limits, to any position that is necessary to make such reduction. It is known as an isochronous governor.

Note that a frequency shift may occur either by variation of the actual frequency, or change in the reference value f_0 , which is accomplished through a change in the pivot point, usually via a screw mechanism, triggered by a "synchronization engine", or change of speed level motor.

Isochronous governors are not used in multiple machines systems, because of the need for appropriate division of load between the machines. The division itself is ensured by providing a regulation and speed decrease in the governor action or speed control (Kundur, 1994).

2.2 Governor with speed drop

Figure 4 shows the schematic of a governor with speed drop or adjustment of equilibrium. The characteristic drop is due to the connection between the pilot valve and the main servo motor

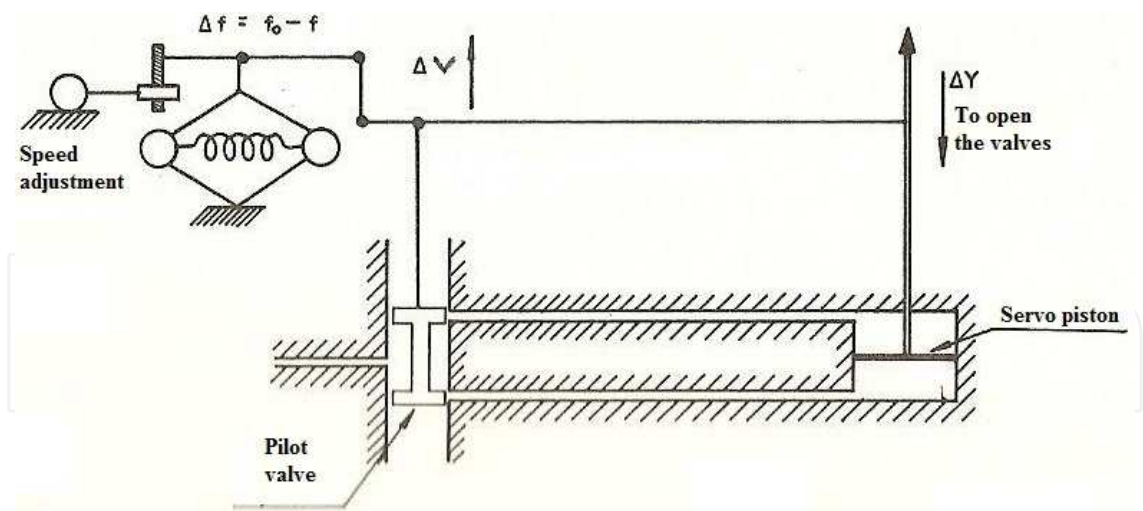


Fig. 4. Schematics of the speed drop governor

With reference to the block diagram of the isochronous governor in figure 2, the effect of the feedback connection, figure 4, is represented by inserting a gain K_3 . This fact is illustrated in figure 5.

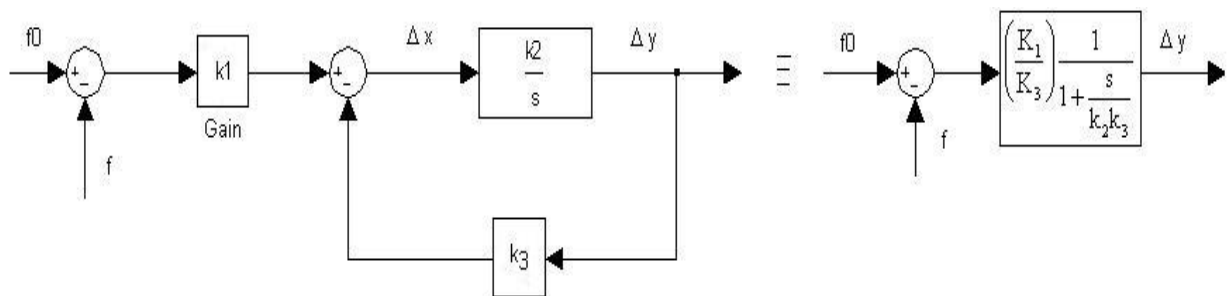


Fig. 5. Block diagram of the governor with speed drop

Figure 6 shows the time response of the valves controlled by the speed governor to a step change in the frequency deviation. TG is known as a time constant of speed governor, usually the order of a fraction of a second (0.5 s).

From the transfer function in figure 6, a function given by equation (4), one can notice that the value of the steady-state frequency shift Δf required to produce a variation of 1 p.u. at the valve of the turbine ΔV is R. This parameter is known as “speed control”.

$$\frac{\Delta \text{valve (p.u.)}}{\Delta \text{frequency (p.u.)}} = \frac{1}{R(1 + sT_G)}$$

(4)

The parameter R can also be expressed in percentage as

$$R\% = \frac{|N_0 - N|}{N_R} \times 100\%$$

where:
 N_0 = speed in steady-state at no load (valves closed);

N = steady-state speed at full load (valves completely opened);
 N_R = rated speed.

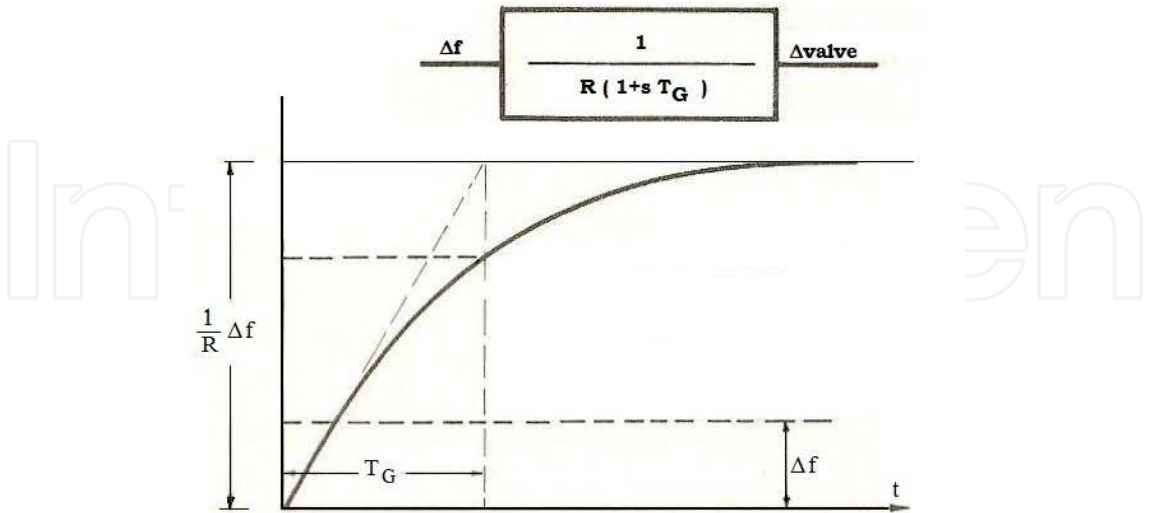


Fig. 6. Throttle response controlled by the speed governor in figure 4 to a step change in the frequency deviation.

Thus, a regulation of 5% means that a frequency deviation of 5% causes a 100% change in power or at the valve outlet. In the terminology of process control, the governor would be characterized as a proportional control of a proportional gain of $1/R$, or a proportional band of $R \times 100\%$.

In order to familiarize the reader with the methodology used to perform computer simulations of dynamic software analysis, it is presented through figure 7 the block diagram of a steam turbine with reheat, figure 7(a) and without reheating, figure 7(b). However, they are representations for a system that is being represented by a single equivalent electric machine.

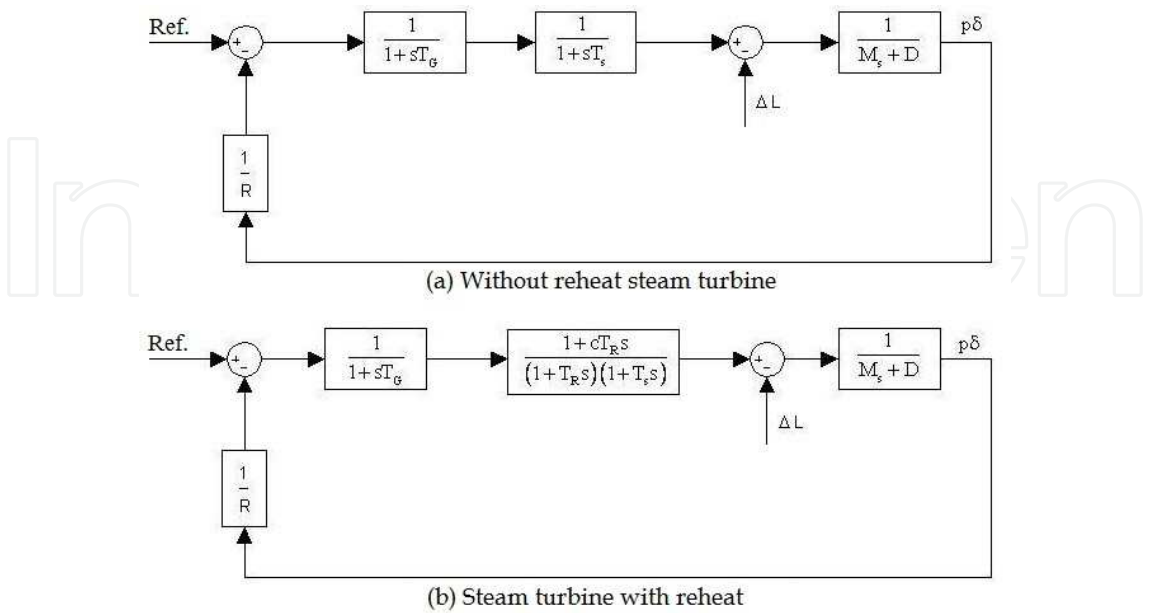


Fig. 7. Block diagrams for isolated systems represented by a single equivalent machine: (a) steam without reheat, (b) steam with reheat

In figure 7 was used the following notation:

$M = \Sigma (MS + MR + MH) =$ combined inertia moment;

$D = \partial PL / \partial \omega =$ damping characteristics of the load;

$R_s =$ Regulation of steam without reheating;

$R_r =$ Regulation of steam with reheating;

$T_R =$ Reheater time constant;

$T_S =$ Charging time of the steam turbine;

$T_G =$ Time constant of the governor.

However, figure 8 presents the block diagram of a steam turbine in a simplified form. It is one of the models adopted by the IEEE – Institute of Electrical and Electronic Engineers (Anderson & Fouad, 2003). It is noteworthy that for a steam unit $T_4 = 0s$.

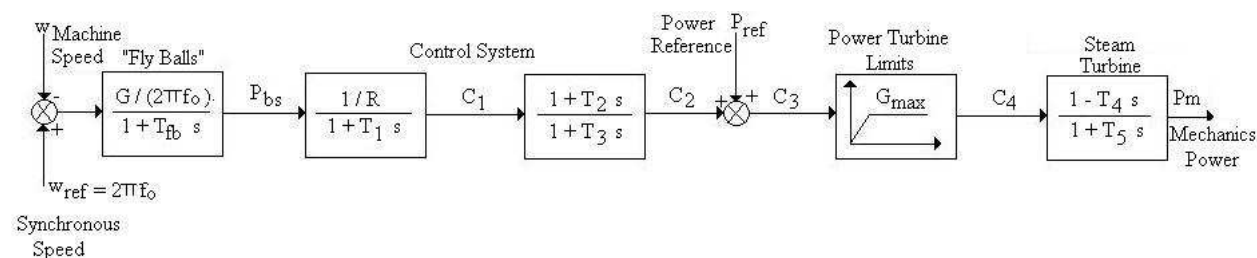


Fig. 8. Model for a thermal turbine speed governor

3. Steam turbine operation under abnormal conditions of frequency

Special attention has been given to the operation of turbo-generators under abnormal system operating conditions concerning the frequency (over or under frequency). In particular, more research efforts have been made to analyze the possible damage the steam turbines are the subject when operating in conditions of prolonged under frequency, during a severe overload imposed on the system with the occurrence of a generation deficit.

To avoid a total collapse of the system and minimize the damage to the equipment during such disturbances, considerable effort has been expended in the development and implementation of automatic load shedding. These load shedding programs are idealized to reject just enough loads to lighten the remaining generation system from overload to restore as soon as possible the system frequency close to nominal.

Both the turbines and generators have operational restrictions, to different degrees, under abnormal frequency conditions. On the other hand, steam turbines are more sensitive to the under frequency phenomena when compared with the attached generators. For this reason, the following discussion is related to the steam turbines (Anderson & Fouad, 2003).

3.1 Turbine limits

The steam turbine consists of a sequence of stages of increasing dimensions with each stage having more complicated geometry of stator and rotor blades. Each blade row has its own natural frequency. The turbines are carefully designed so that the resonance frequencies of the blades to the rated speed are sufficiently out of phase, to avoid vibration and excessive “stress” or fatigue.

Must be highlighted that here will be presented a discussion for systems operating in a nominal frequency of 60 Hz, like in Brazil.

Figure 9 illustrates the phenomenon that involves operations of the turbines under off-nominal frequency ("off-frequency operation"), showing the amplitude of vibrations fatigue for a number of stages of a turbine vane according to the nominal frequency. It is observed that when the turbine operates out of its nominal frequency, the amplitude of "stress" increases and some damage can be cumulative.

The Campbell diagram, illustrates how a change in turbine speed can provide steam excitation frequencies that coincide with the natural frequencies of a blade, how can be seen in the reference cited at final of this paragraph. At the figure 9 is demonstrated the relationship between blade failure due to fatigue and off-frequency operation. Below stress level A, the vibration stress amplitude is low enough that no damage results. Operation at stress level B would produce a failure at 10^4 cycles, and at level C failure would occur at 10^3 cycles (Kundur, 1994).

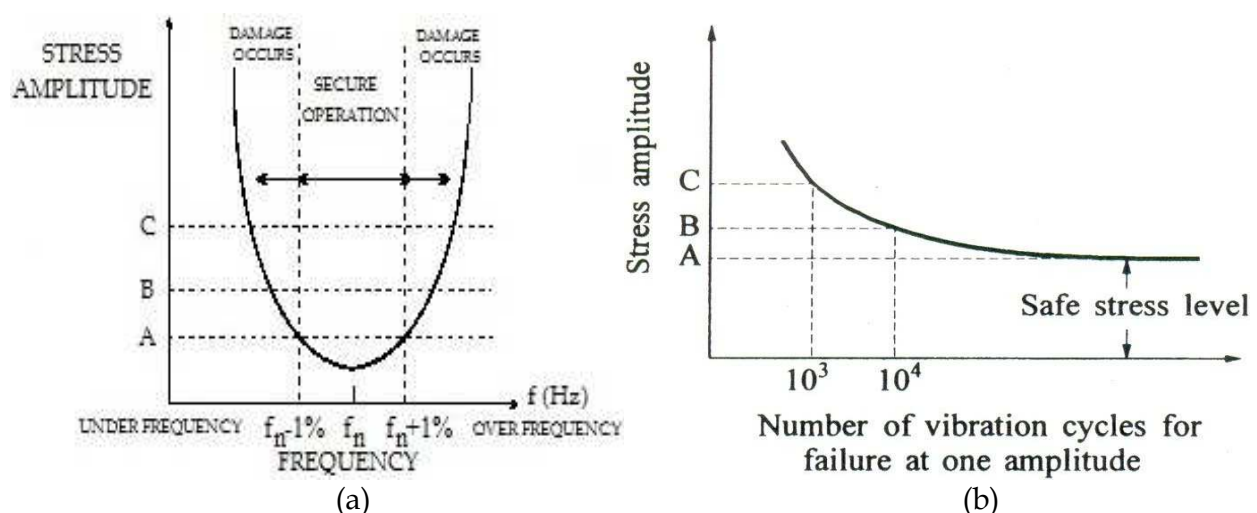


Fig. 9. Frequency x stress (fatigue) range for steam turbines (a) Increase in vibration amplitude with off-frequency operation; (b) Stress x number of cycles to failure

Research for a large amount of vibration frequency data leads to the time limits suggested for operations outside of the nominal frequency range and for different steam turbines that are represented in figure 10.

The diagram of figure 10 represents the estimated minimum time to the failure of some part of the structure of the blades, illustrating the limits of time for operation of steam turbines for both the under-frequency and for over-frequency. It is observed for a frequency deviation of 5% or more, the damage time becomes very small and it is not practical to operate a system more than a few seconds in this frequency range.

As can be seen, for the lower limit frequency, i.e., approximately $f_n - 6\%$ Hz (see figure 10), the permissible minimum time is one second for frequencies near the nominal time is undefined so that a variation frequency of $\pm 1\%$, will have no harmful effect on the blades.

It is important to note that the effect of operation outside the nominal frequency is cumulative, i.e., half a minute of operation under full load at $f_n - 4\%$ Hz now leaves only approximately another half a minute of $f_n - 4\%$ Hz for operation in the unit life.

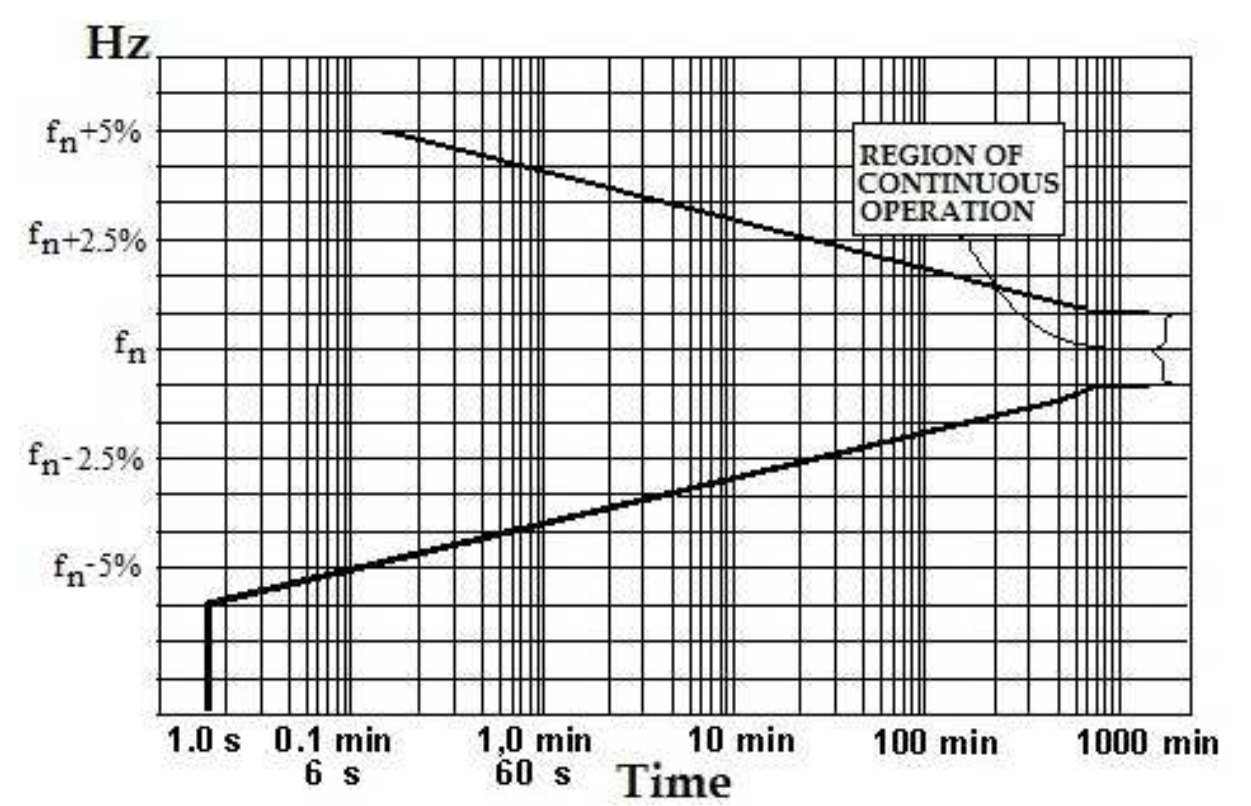


Fig. 10. Frequency limits of the operation of a steam turbine

From figure 10, we can build table 1 that shows the maximum time values of operating a steam turbine according to its frequency.

Frequency at full load (Hz)	Maximum operating time
$f_n - 1\%$	Continuously
$f_n - 2\%$	100 minutes
$f_n - 3\%$	10 minutes
$f_n - 4\%$	1 minute
$f_n - 5\%$	0.1 minute
$f_n - 6\%$	1 second

Table 1. Maximum operating time of a steam turbine according to its frequency of operation at full load

The condition most often found corresponds to the turbine over-frequency, resulting in sudden shutdown of the generator by the action of the breaker. Under these conditions the characteristic of the speed governor will allow an over speed of around 5% and from there take immediate action to reduce the speed to close to the nominal (Anderson & Fouad, 2003).

3.2 Cascading shots

If a limit is reached for operating a turbine, it will be disconnected from the system by actions of its protection. This exacerbates the problem, since the power imbalance increases (greater deficit of generation), and consequently, the frequency drops quickly and the system enters a cascade process until it comes to the collapse.

Thus, we can define three characteristic zones of frequency for operation of turbines, as shown in table 2.

OPERATION ZONE	FREQUENCY - f (Hz)
Favorable	$f_n - 0.17\% < f_n < f_n + 0.17\%$
Tolerable	$f_n - 1\% < f_n < f_n + 1\%$
Extreme	$f_n - 6\% < f_n < f_n + 1.7\%$

Table 2. Characteristic zones of frequency for operation of turbines

The zone limits are practical, because they were obtained empirically. Table 2 indicates a favorable frequency zone of (60±0.1) Hz. As a reference, in the USA the limits are of the order of (60±0.05) Hz.

Figure 11 shows the characteristic ranges or zones of frequencies (based on Table 2) and the minimum values that can cause damage in the operation of steam turbines.

For this reason, emphasis is given to methods to protect the turbine under-frequency conditions, and to this end, a system must be equipped with a load shedding program, and this requires a prior knowledge of the system behavior.

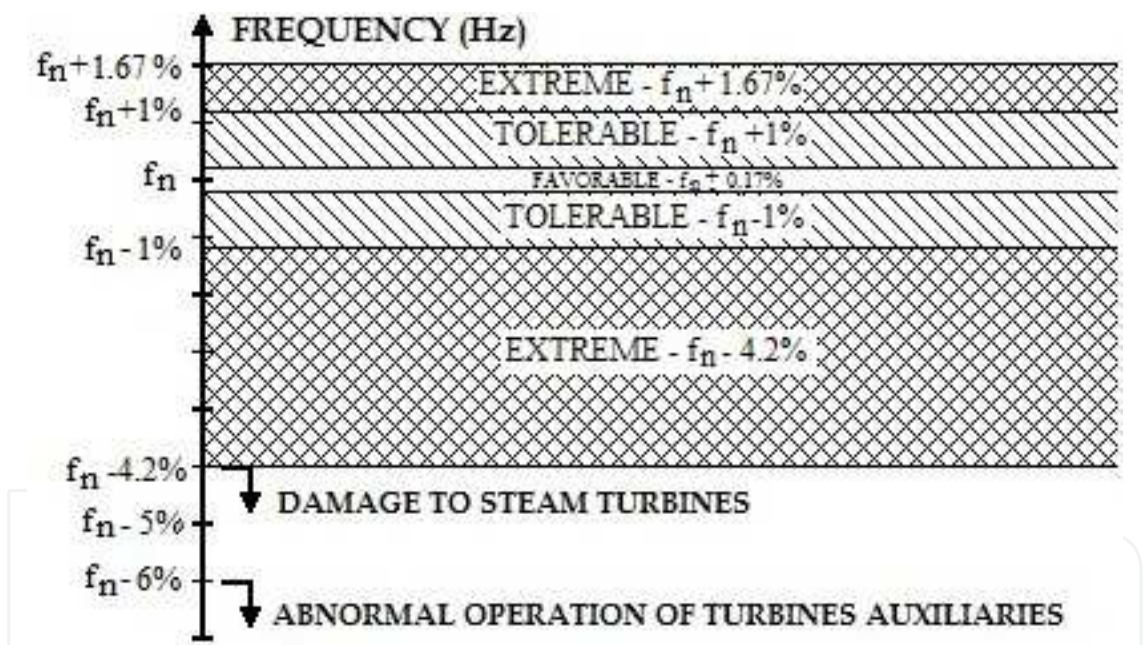


Fig. 11. Effect of frequency on the operation of the turbines

4. Case study

In order to assess the impacts on the steam turbine blades of a thermal unit, which steam is originated by the burning of bagasse and cane sugar straw, it is used the electrical system depicted in Figure 12 below.

Figure 12 illustrates the single line diagram of the electrical system to be used as reference for the study to be conducted. This single line diagram is very representative of the typical condition of independent generation interconnected with a larger electrical system. It is an

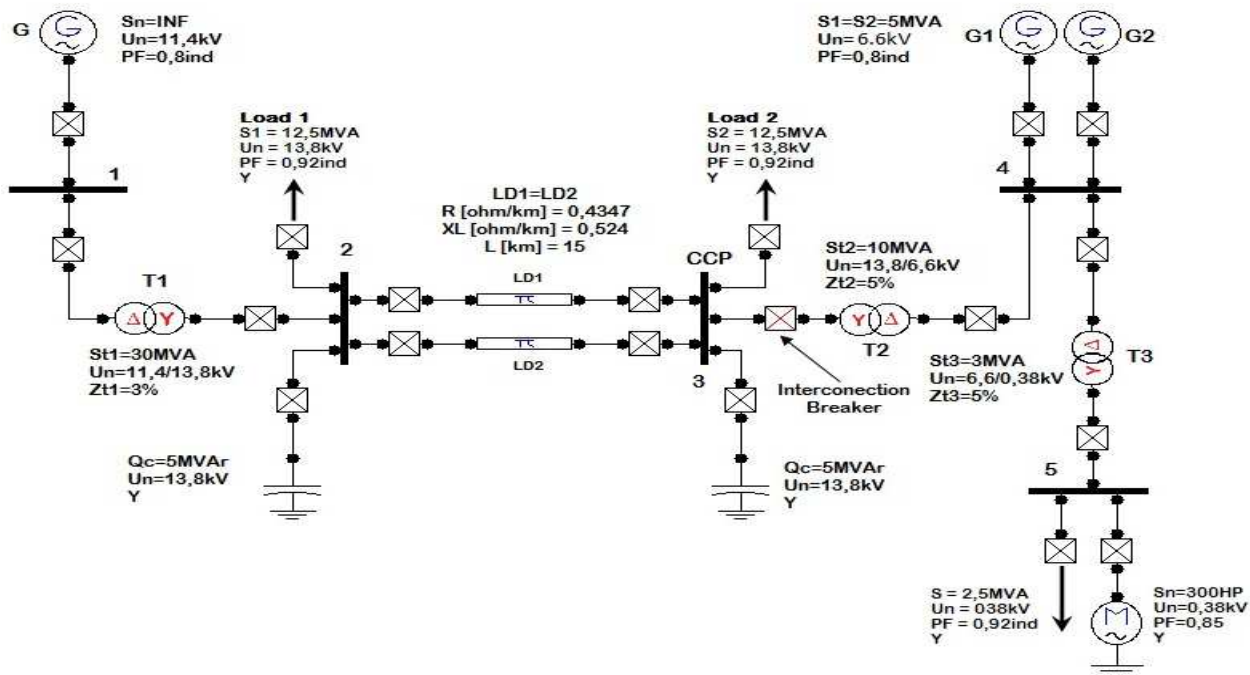


Fig. 12. Single line diagram for the electrical system in the case considered

electricity distribution network, connected to the busbar number 3 (Point of Common Coupling - PCC), through a transformer, the independent producer electrical system. The representation of the (IPP) Independent Power Producer consists of two synchronous generators (whose primary machines are steam turbines), a static electrical load as well as an electric motor, internal to this “independent” system. In addition to meeting its domestic demand for energy, these generators also provides power to the distribution network.

The three-phase distribution network has an ideal voltage source (infinite bus), connected to transformer T1, through busbar 1. This transformer T1 is connected to two power distribution lines of 13.8 kV through busbar 2. This busbar has a capacitor bank and load. The two referred distribution lines end at busbar 3, where it is connected to transformer T2. At busbar 3, there is a bank of capacitors and load. Transformer T2 is used to make the connection between the power utility and the independent power producer. The transformer T2 is also connected to busbar 4, where are connected the generators of the independent power producer (IEEE Std. 1547, 2003). These generators have the nominal values of 5 MVA, 6.6 kV. At busbar 4 there is also another transformer T3, which is connected to busbar 5, where we have the loads of the independent power producer.

The voltage source, which is the mains of the distribution system, was implemented as na ideal three-phase source. Therefore, the short-circuit level at busbar 1 is considered infinite.

The data needed for modeling the independent power producers generators (among others, the sub-transient, transient, synchronous reactance and time constants) are listed in Table 3.

The rated parameters obtained for the machine voltage and speed regulators, as well as data referred to the independent power producer synchronous generator, were obtained directly from manufacturers.

Data needed for G1 (G1 = G2)	
$S_n = 5MVA$	$x_0=0.046pu$
$U_n= 6.6kV$	$T'_{d0}=1.754s$
$R_A= 0.004pu$	$T'_{q0}=0s$
$x_L= 0.1pu$	$T''_{d0}=0.019s$
$x_d= 1.8pu$	$T''_{q0}=0.164s$
$x_q=1.793pu$	$H_1=1s ;H_2=2s$
$x'_d=0.166pu$	$P=4\text{ poles}$
$x'_q=0.98pu$	$f=60\text{ Hz}$
$x''_d=0.119pu$	$\omega_s = 188.5\text{ rad/s}$
$x''_q=0.17pu$	---

Table 3. Synchronous machine parameters for the independent generator

It is highlighted that this independent generator is driven by a steam turbine with regulators and governors modeled in “ATP-Alternative Transients Program”, through the use of TACS subroutines. Thus we adopted here the block diagram shown in Figure 8 in order to assess the dynamic response of the system of Figure 12, towards the contingency to be applied. Similar works using ATP were developed like (Saldaña et al., 2006) and an important work about distributed generation can be found in through (Freitas et al. 2006).

However, it is necessary the modeling of the voltage regulator to obtain a better and more reliable response from the model. In this way, it is presented through Figure 13 the block diagram used to represent the excitation regulator. This is the IEEE type I model (Guimarães, 1990).

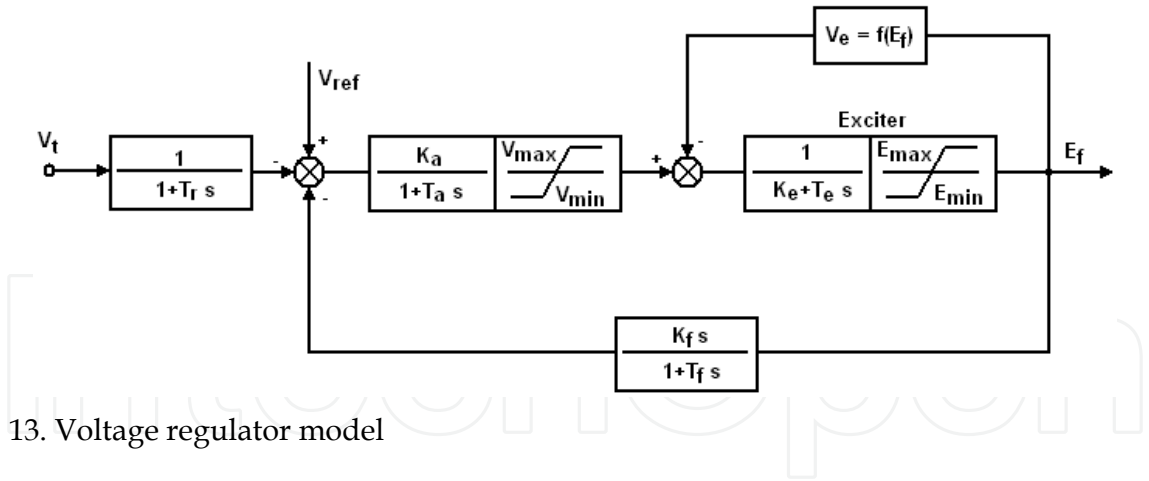


Fig. 13. Voltage regulator model

4.1 Sudden opening of the interconnection breaker

With the purpose of evaluating the influence of penetration of the independent power producer in the largest network and its close correlation with the inertia moment of the generator, with regard to the maintenance of transient stability was established the power flow illustrated in Table 4.

The machines of the IPP generate a total of 4.2 MW and 1.5 MVA_r respectively of active and reactive three-phase power. Thus, the total of active power generated 1.7 MW is designed to the grid of the local electricity authority.

Source	P _G [MW]	Q _G [MVA _r]
G1	0.7	0.25
G2	0.7	0.25

Table 4. Active and reactive power generated by the independent power sources

It is worth clarifying to the reader the pre-established conditions to the speed governors of the IPP machines, these were adjusted to operate with a 5% slope, in order to better meet the interconnection. Therefore, no machine installed in the IPP generation, has the characteristic to ensure that frequency oscillations will be inside the favorable frequency range, i.e., there is no need for the presence of an isochronous generator.

Faced by the sudden opening of the interconnection circuit breaker there is a considerable fluctuation in the speed of the electric machine G2, Figure 14(a). Such transient oscillation immediately affects the frequency in the electrical system belonging to the IPP, burdening strongly the quality of electricity, especially with regard to the efficiency of micro-computerized devices (Dugan et al., 2002).

However, slight changes in the operating speed of the machines originate variations in power demand, since the active and reactive powers, required by electrical loads vary dynamically with system frequency. Nevertheless, there is clearly and strongly the tendency of the synchronous machine speed G2 to stabilize, as shown in Figure 14(a) in the period after contingency, thus indicating the influence of the IPP generation penetration in the transient stability of its own machines.

As for the speed regulator, Figure 14(b) convincingly portrays the attempt of that regulator to meet the new situation imposed on the system.

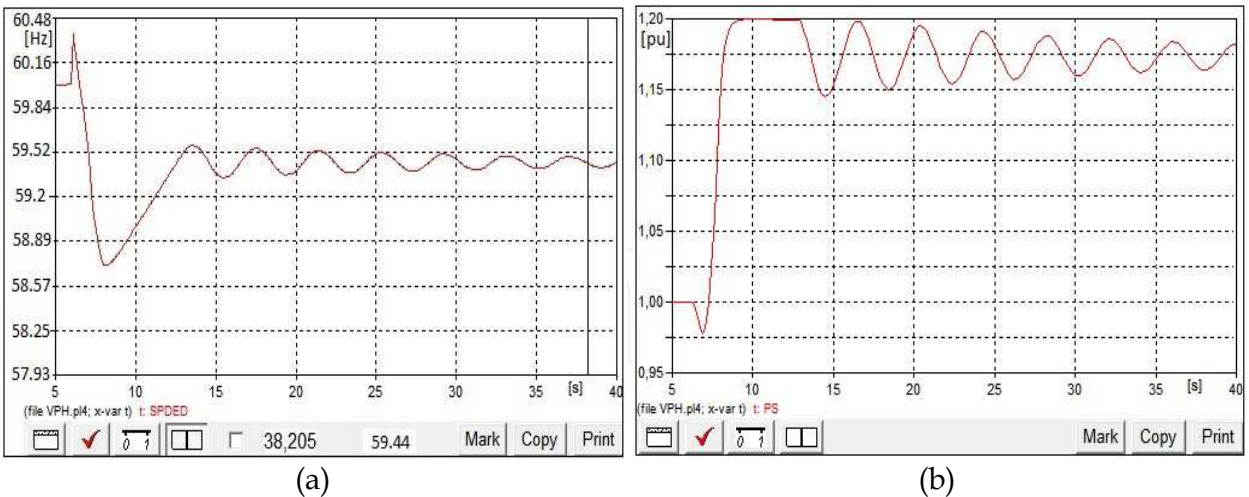


Fig. 14. Response of the mechanical variables of the generator G3 (a): Operating frequency; (b) Action of the speed governor

In the moment immediately after the opening of the interconnection breaker, the machine is subjected to an immediate rejection of load. Thus, the operating speed rises gently to 189.63 rad/s ($f = 60.4$ Hz). However, at this moment the lower inertia machine G1 is taken out of the system, in order to restore the load-generation balance. It is worth mentioning the

performance of the machine G2 speed regulator in Figure 14(b) to reduce the steam consumption to ensure the G2 synchronous speed.

With the withdrawal of G1, a new scenario is presented with respect to the power flow in the system. The machine G2 becomes responsible for all the electrical loads at the IPP. Thus, according to equation (5), the balancing equation, the electrical power becomes greater than the mechanical power, which leads to deceleration of the generator, taking the angular speed to $\omega = 184.45 \text{ rad/s}$ ($f = 58.71 \text{ Hz}$). At this moment, the speed governor acts to increase the steam consumption to restore the load-generation balance. However, the frequency of operation of the machine oscillates in a damped transient between $f_1 = 59.6 \text{ Hz}$ ($\omega = 187.15 \text{ rad/s}$) and $f_2 = 59.33 \text{ Hz}$ ($\omega = 186.42 \text{ rad/s}$), and tends to stabilize at a frequency $f = 59.4 \text{ Hz}$, i.e., $\omega = 186.74 \text{ rad/s}$.

$$\frac{2H.d^2\delta}{\omega_R.dt^2} = P_m - P_e = P_a \quad (5)$$

As for the speed governor, it follows the oscillations observed in the operating speed of the machine G2, tending to stabilize around 1.17 pu, in other words, it is necessary the production by the boilers of 17% more steam, to be supplied to the generators turbine to meet the new request of active power, as can be observed in Figure 14(b).

The moment immediately after the withdrawal of the machine G1, the remaining generator G2 reaches the frequency $f = 58.71 \text{ Hz}$. That is classified as extreme in Table 2, burdening sharply the impeller blades of this generating set. However, during the damped transient period, G2 oscillates within the tolerable region of Table 2. The observation of such limits ensures the life time of the equipment, thus reducing the mechanical wear of turbine blades and reduces the number of stoppages for maintenance of this generating set.

In order to get a better response in operation for the IPP electrical system after the opening of the interconnection circuit breaker, it is possible the insertion of a flywheel in the axis of G2, in order to rise the generating set equivalent inertia.

However, it is necessary to reject the generating unit G1 inside the 100 ms after the application of contingency.

4.2 Application of a flywheel

The flywheel is a mechanical device with significant moment of inertia used for storing rotational energy. Has high resistance to variations in speed, which helps to ensure a small variation in rotation speed of the shaft (Kundur, 1994).

The energy is stored in the rotor as kinetic energy, or more specifically, rotational energy:

$$E_k = \frac{1}{2}.I.\omega^2 \quad (6)$$

where:

- ω is the angular speed, and
- I is the mass moment of inertia about the center of rotation.

An increase in angular speed greatly increases the energy stored in the flywheel, and the energy density of the KESS – Kinetic Energy Storage System. However, the no-load losses, viscous friction with air and by contact and friction in mechanical bearings, will be higher, hurting the efficiency of the system. In addition, the rotating parts of the system must support high mechanical stresses due to high speed at which they are submitted. These limitations found in KESS can now be properly solved because:

- the development of new materials such as fiberglass and carbon;
- the use of vacuum systems, which reduce the losses by viscous friction with the air;
- the use of magnetic bearings that eliminate friction by contact;
- the advancement of power electronics, which improved signal conditioning;
- the evolution of microelectronics, that allowed more sophisticated and less expensive control systems.

These factors enable the development and implementation of a new generation of KESSs, with superior performance, whose speed can reach tens of thousands of rpm (approximately 60,000 rpm). Thus, increases the number of possibilities for the use of flywheels, since this generation presents high energy density and power.

Among the applications for this equipment, we can mention:

- uninterruptible power supply (UPS systems);
- provision of extra energy in case of increased demand;
- compensation of voltage dips.

The moment of inertia is a measure of resistance to the applied torques in a rotating object, i.e., the higher the moment of inertia, the slower the wheel will spin after applying a certain force on its axis.

It is presented here the main ways to obtain the moment of inertia for a solid cylinder:

$$I = \frac{1}{2} \cdot m \cdot r^2 \quad (7)$$

However, for an empty cylinder with thin walls, one must employ the equation (8) detailed below:

$$I = m \cdot r^2 \quad (8)$$

However, in the case of an empty cylinder with thick walls, one should use the equation 9 below:

$$I = \frac{1}{2} \cdot m \cdot (r_1^2 + r_2^2) \quad (9)$$

Where m is the mass and r is the radius of gyration.

It is worth to present equation (10) used to obtain the constant of inertia of a generator.

$$H = \frac{\frac{1}{2} \cdot \omega_s^2 \cdot I}{S_n} \quad (10)$$

In a simplified perspective, the procedure is the analysis of the flywheel shown in Figure 15.

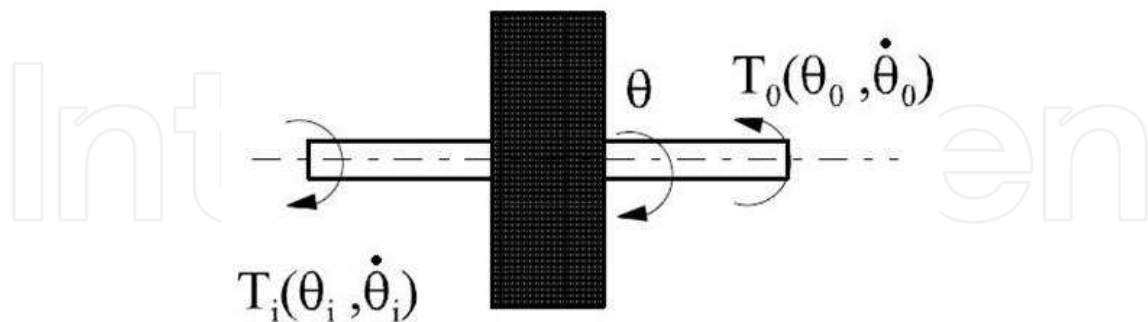


Fig. 15. Simplified representation of a flywheel.

Where:

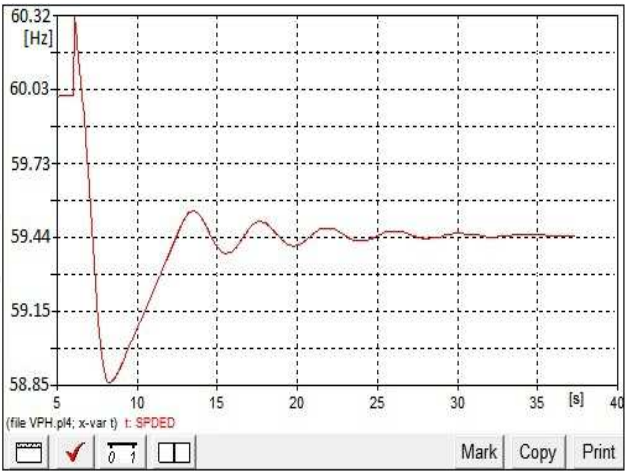
- I is the inertia moment of the wheel;
- θ is the wheel angular position;
- T_i corresponding torque to an angular position θ_i ;
- T_o corresponding torque to an angular position θ_o ;
- $\dot{\theta}_i$ angular speed at the angular position θ_i ;
- $\dot{\theta}_o$ angular speed at the angular position θ_o .

Taking, arbitrarily, the torques T_i and T_o as a positive and negative, respectively, we get the equation for the motion of the wheel:

$$M = T_i(\theta_i, \dot{\theta}_i) - T_o(\theta_o, \dot{\theta}_o) - I \ddot{\theta} = 0 \quad (11)$$

It is presented here different situations for three specific inertia moments, and their corresponding implications on the speed response of the IPP generator G2 in Figure 16.

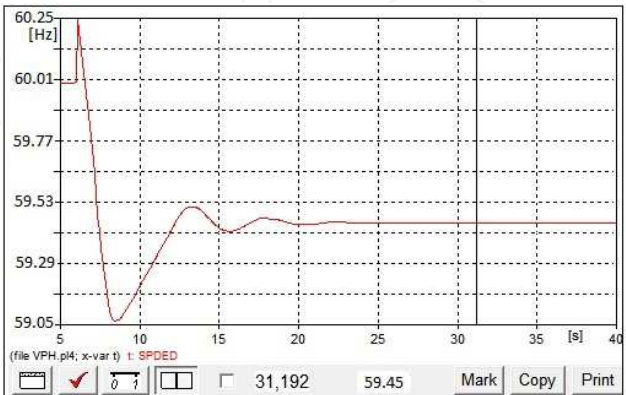
With the increase in the synchronous machine G2 equivalent moment of inertia, due to the insertion of a wheel, in Figure 16(a) for $I = 600 \text{ kgm}^2$, there is the stabilization of the operating speed of the generator for the considered time period in the simulation at $t = 40\text{s}$. However, at the moment immediately after the untimely opening of the interconnection breaker, the operating speed of machine G2 reaches $\omega = 189.5 \text{ rad/s}$ ($f = 60.3 \text{ Hz}$). This is due to the instantaneous rejection of the applied load. Nevertheless, due to the withdrawal of machine G1, G2 provides a considerable reduction in its speed of operation due to the increase in electric power demand. The frequency reduces to 184.93 rad/s ($f = 58.9 \text{ Hz}$), the extreme region of operation according Table 2. However, the machine varies in speed within the range between $186.53 < \omega < 187.07 \text{ rad/s}$, or $59.4 < f < 59.5 \text{ Hz}$. Note that, observing Table 2, the oscillation frequency remains within the favorable zone of operation, ensuring the life time of steam turbine blades.



(a)



(b)



(c)

Fig. 16. Frequency response of machine G2 for different inertia moments (a): $I = 600 \text{ kgm}^2$; (b): $I = 700 \text{ kgm}^2$; (c): $I = 800 \text{ kgm}^2$

Figure 16(b) shows the response to an equivalent moment of inertia $I = 700 \text{ kgm}^2$. The system has more damping, reducing the time required to reach a new steady state speed at $\omega = 186.77 \text{ rad/s}$ ($f = 59.5 \text{ Hz}$). Therefore, according Table 2, the industrial frequency falls in the tolerable operating zone, contributing not only to maintain the transient stability of the system, but also ensures the integrity of the steam turbine blades, as well as presenting a significant contribution in terms of the quality of electric power. As for the oscillations of frequency in the transient period, it is verified a maximum speed of $\omega = 189.4 \text{ rad/s}$ ($f = 60.3 \text{ Hz}$), at the moment immediately after the contingency. Nevertheless, with the removal from operation of G1, machine G2 reaches a minimum speed of $\omega = 185.28 \text{ rad/s}$ ($f = 59.0 \text{ Hz}$) at the extreme operation zone.

However, the machine G2 varies in speed within the range between $186.61 < \omega < 187.01 \text{ rad/s}$ or $59.4 < f < 59.5 \text{ Hz}$. It can be noticed that the frequency oscillation, according Table 2, remains in the favorable zone of operation, ensuring the expected life time for blades of the steam turbine.

With the main objective to reduce the oscillations, evident in the speed of operation, of the remaining synchronous generator (G2) it was applied an equivalent moment of inertia $I = 800 \text{ kgm}^2$, the result can be seen in Figure 16(c). There, the damping obtained allows reaching the new steady state more efficiently. This helps to mitigate the harmful effects to the quality of electric power to ensure better response of electrical parameters of the system.

With regard to changes in speed, the maximum reaches the magnitude $\omega = 189.3 \text{ rad/s}$ ($f = 60.3 \text{ Hz}$) at the tolerable zone of operation, but the minimum is settled at $\omega = 185.55 \text{ rad/s}$ ($f = 59.06 \text{ Hz}$) at the extreme operation zone. Thus, one can conclude here and for the other equivalent inertia moments simulated that, at the instant immediately after the removal of generator G1, the synchronous machine G2 presents a significant reduction in its operating speed. In this way, it is generated a sub-frequency costly to the physical and mechanical integrity of the turbine blades, since the obtained frequency, at this instant, fits the extreme region of operation at Table 2. However, oscillations in the transient period do not affect the impeller blades, as they pass inside the tolerable zone. Nevertheless, after the damped transient period, the machine reaches the new steady-state and stabilizes at a speed $\omega = 186.77 \text{ rad/s}$ ($f = 59.5 \text{ Hz}$), similar to that obtained for the case illustrated in Figure 16(b).

5. Conclusion

Through the discussions presented along this chapter, there is the need to make the correct and effective study of the synchronous machine speed governors, in order to obtain better dynamic response of the system. However, this goal is achieved from the transfer function of these governors, so it is essential to be aware of the topology of the turbine used, i.e., whether or not this is reheating. It shows that before the model transfer function, yet it is necessary to choose an appropriate software to implement the model. In this way, it can be seen that ATP, through TACS subroutines allows the correct and efficient computational modeling of both the speed governor and voltage regulator.

The answers regarding the performance of the speed governor, for the transfer function shown here, respond faithfully and reliably to dynamical requests imposed to the electrical system under analysis.

Due to untimely performance by interconnection break, the IPP machines face an immediate rejection of load, which burdens the system frequency, thereby compromising the integrity of turbine blades. However, it appears that even without the application of mitigation measures the system tends to stabilize. Nevertheless, the responses refer to a system such that the penetration of IPP does not take place significantly. The literature shows that higher levels of active power exported by the IPP mean larger damage to the turbines due to higher frequency oscillations. Thus, the use of the flywheel is shown as an effective alternative, since it damps transient oscillations, thus contributing to ensuring the life time of the impeller blades.

In short, it is extremely important the correct modeling and use of speed governors in studies relevant to the dynamic stability of power system analysis in terms of commitment to the life time of the blades of steam turbines.

6. References

- Moura, F. A. M. ; Camacho, J. R. ; Chaves, M. L. R. & Guimarães, G. C. *"The Dynamic Interaction of Independent Power Producer Synchronous Machines Connected to a Distribution Network in ATP-EMTP"*, ICEM2010 – XIX International Conference on Electrical Machines, Rome, Italy, September 2010.
- Moura, F. A. M. ; Camacho, J. R. ; Chaves, M. L. R. & Guimarães, G. C. *"Independent Power Producer Parallel Operation Modeling in Transient Network Simulations for Interconnected Distributed Generation Studies"*, Electric Power Systems Research, Elsevier, Article in Press, (2009),doi:10.1016/j.epsr.2009.08.016.
- Anderson, P. M. & Fouad, A. A. *Power System Control and Stability*, vol. I. Iowa, 1977.
- Kundur, P. *Power Systems Stability and Control*, McGraw-Hill, EPRI Power Systems Engineering Series, New York, 1994.
- IEEE Standard for Interconnecting Distributed Resources with Electric Power Systems, IEEE Std. 1547, New York, USA, 2003.
- LIPA-Long Island Power Authority, *Control and Protection Requirements for Independent Power Producers, Transmission Interconnections*, found at the internet in 22/11/2007, at <http://tinyurl.com/33clq4>.
- Saldaña, C. ; Calzolari, G. & Cerecetto, G. *"ATP modeling and field tests of the ac voltage regulator in the Palmar hydroelectric power plant"*, Electric Power Systems Research, Elsevier, 76 (2006), pp.681-687.
- Freitas, W. ; França, A. M.; Vieira Jr., J. C. M. & Silva, L. C. P. *"Comparative Analysis Between Synchronous and Squirrel Cage Induction Generators for Distributed Generation Applications"*. IEEE Trans. Power Systems, vol. 21,NO.1, FEBRUARY 2006.
- Guimarães, G. C. *Computer Methods for Transient Stability Analysis of Isolated Power Generation Systems with Special Reference to Prime Mover and Induction Motor Modelling*, PhD Thesis, University of Aberdeen, 1990.

Dugan, R. C. ; McGranaghan, M. F. ; Santese, S. & Beaty, H. W. *Electrical Power Systems Quality*, McGraw-Hill, New York, 2002.

IntechOpen

IntechOpen



Mechanical Engineering

Edited by Dr. Murat Gokcek

ISBN 978-953-51-0505-3

Hard cover, 670 pages

Publisher InTech

Published online 11, April, 2012

Published in print edition April, 2012

The book substantially offers the latest progresses about the important topics of the "Mechanical Engineering" to readers. It includes twenty-eight excellent studies prepared using state-of-art methodologies by professional researchers from different countries. The sections in the book comprise of the following titles: power transmission system, manufacturing processes and system analysis, thermo-fluid systems, simulations and computer applications, and new approaches in mechanical engineering education and organization systems.

How to reference

In order to correctly reference this scholarly work, feel free to copy and paste the following:

Fabício A. M. Moura, José R. Camacho, Geraldo C. Guimarães and Marcelo L. R. Chaves (2012). Steam Turbines Under Abnormal Frequency Conditions in Distributed Generation Systems, Mechanical Engineering, Dr. Murat Gokcek (Ed.), ISBN: 978-953-51-0505-3, InTech, Available from:
<http://www.intechopen.com/books/mechanical-engineering/steam-turbines-under-abnormal-frequency-conditions-in-distributed-generation-systems>

INTECH
open science | open minds

InTech Europe

University Campus STeP Ri
Slavka Krautzeka 83/A
51000 Rijeka, Croatia
Phone: +385 (51) 770 447
Fax: +385 (51) 686 166
www.intechopen.com

InTech China

Unit 405, Office Block, Hotel Equatorial Shanghai
No.65, Yan An Road (West), Shanghai, 200040, China
中国上海市延安西路65号上海国际贵都大饭店办公楼405单元
Phone: +86-21-62489820
Fax: +86-21-62489821

© 2012 The Author(s). Licensee IntechOpen. This is an open access article distributed under the terms of the [Creative Commons Attribution 3.0 License](https://creativecommons.org/licenses/by/3.0/), which permits unrestricted use, distribution, and reproduction in any medium, provided the original work is properly cited.

IntechOpen

IntechOpen